Eur. J. Biochem. **268**, 2301–2307 (2001) © FEBS 2001

Assignment of the disulfide bonds of huwentoxin-II by Edman degradation sequencing and stepwise thiol modification

Qin Shu[1], Renhuai Huang[2] and Songping Liang[1,2]

[1]*Life Sciences College, Peking University, Beijing, China;* [2]*Life Sciences College, Hunan Normal University, Changsha, China*

A novel strategy combining Edman degradation and thiol modification was developed to assign the three disulfides of huwentoxin-II (HWTX-II), an insecticidal peptide purified from the venom of the spider *Selenocosmia huwena*. Phenylthiohydantoin (Pth) derivatives of Cys and the elimination product, dehydroalanine (ΔSer), can be observed in the Cys cycles during Edman degradation of native HWTX-II. The appearance of two products indicates that the disulfides of HWTX-II were split and that the free thiol group of the second half cystine has been generated. Information about the nature of the disulfide bridges of HWTX-II could be obtained from the sequencing signal if the nascent thiols were modified stepwise by 4-vinylpyridine. Using this method the disulfide bridges of HWTX-II were assigned as Cys4–Cys18, Cys8–Cys29 and Cys23–Cys34, which is different from that seen in HWTX-I, a neurotoxic peptide from the same spider. Using this strategy, one can assign the disulfide bonds of small proteins by sequencing and modification $n - 1$ times, where n is the number of disulfide bonds in the protein. The above assignment of the disulfide bonds of HWTX-II was confirmed by MALDI-TOF MS of tryptic fragments of HWTX-II. Some disulfide interchanging during proteolysis was observed by monitoring the kinetics of proteolysis of HWTX-II by MALDI-TOF MS.

Keywords: huwentoxin-II; disulfide bond; Edman degradation sequencing; thiol modification; MALDI-TOF MS

HWTX-II is an insecticidal peptide purified from the venom of the spider *Selenocosmia huwena*. It can paralyze cockroaches reversibly for several hours, with an effective dose (ED_{50}) of 127 ± 54 $\mu g \cdot g^{-1}$, and act cooperatively to potentiate the activity of HWTX-I to block neuromuscular transmission in isolated mouse phrenic nerve diaphragm preparations [1]. HWTX-II contains 37 amino-acid residues including six cysteines that form three disulfide bonds. The primary structure of HWTX-II is highly homologous with ESTX, a toxin from the American tarantula spider *Eurypelma californicum* [2] and venom protein 1 from the Mexican red knee tarantula spider *Brachypelma smithii* [3] (Fig. 1).

It has been found that some of the peptide components from spider venom shared common tertiary structures, known as cystine knot motifs, despite their dissimilar primary structures and biological functions. The core structures of these peptides are dictated more by their disulfide bonding patterns than by their amino-acid sequences [4–6]. Thus the correct assignment of disulfide bonds is essential for determining the structure models and for interpreting the relationship between the structure and function of the molecule. For these reasons we investigated the disulfide bonds of HWTX-II.

Knowing the amino-acid sequence of HWTX-II, we tried to digest the molecule with trypsin and chymotrypsin. The resulting fragments were analyzed by conventional mass spectrometric and Edman sequencing methods. However, as it is difficult to cleave between Cys4 and Cys8 (Fig. 1), and as fragments containing Cys23 and Cys29 are similar, reliable assignment of the disulfide linkages was not possible, especially as some disulfide scrambling of fragments produced in proteolysis was observed.

The reducing reagent, tris(2-carboxyethyl)-phosphine (TCEP) can partially reducing disulfide proteins sample under acidic conditions and has often been used in disulfide structure determinations [7–10]. However, preliminary experiments using reduction with HWTX-II (Q. Shu & S. P. Liang, unpublished results) still led to ambiguities because of disulfide scrambling problems.

During conventional Edman sequencing of intact, non reduced HWTX-II, both Pth–Cys and Pth–ΔSer were observed in the HPLC chromatograms of the Cys cycles. This observation suggested that half cystine anilinothiazolinone (ATZ) formed at this cycle decomposed partly by elimination to form Pth–ΔSer and partly by cleavage of the disulfide bond to form Pth–Cys [11]. The formation of Pth–Cys from one half of the cystine residue implies the production of a free thiol group in the other half cystine residue still in the unsequenced portion of HWTX-II. If the nascent thiol could be modified before further sequencing, a message concerning the identity of the disulfide partners could be obtained from the sequencing signal. From the foregoing, a strategy combining Edman degradation sequencing and thiol modification *in situ* was developed which allowed assignment of the disulfide linkages pattern

Correspondence to S. Liang, Life Science College, Hunan Normal University, Changsha, Hunan 410081, China. Fax: + 86 7318861304, E-mail: liangsp@public.cs.hn.cn

Abbreviations: HWTX-II, huwentoxin-II; Pth, phenylthiohydantoin; PECys, *S*-pyridylethyl-cysteine; AP, aminopropyl; EDC, 1-(3-dimethylaminopropyl)-3-ethylcarbodiimide hydrochloride; AcCN, acetonitrile; 4-VP, 4-vinylpyridine; CCA, α-cyano-4-hydroxycinnamic acid; TCEP, tris(2-carboxyethyl)-phosphine; ATZ, anilinothiazolinone; Tos-Phe-CH_2Cl, *N*-α-tosyl-L-phenylalanylchloromethane; CSH motif, cystine-stabilized α-helical motif; ED, effective dose.

(Received 17 November 2000, revised 15 February 2001, accepted 16 February 2001)

Fig. 1. Alignment of HWTX-II with related proteins. TX4K_EURCA and TXP1_BRASM are the Swissprot database ID codes for ESTX (from *Eurypelma californicum*) and venom protein1 (from *Brachypelma smithii*), respectively. Gaps have been inserted to achieve the best alignment. Strictly conserved residues have a black background, and those with conservative mutations, a grey background.

of HWTX-II and should be generally applicable to similar proteins.

MATERIALS AND METHODS

Chemicals

All sequencing reagents were from Applied Biosystems Division of PerkinElmer. Aminopropyl (AP) glass beads, 4-vinylpyridine (VP), *N*-α-tosyl-L-phenylalanylchloromethane (Tos-Phe-CH_2Cl)/trypsin, chymotrypsin, and α-cyano-4-hydroxycinnamic acid (CCA) were purchased from Sigma. 1-(3-Dimethylaminopropyl)-3-ethylcarbodiimidehydrochloride (EDC) and tris(2-carboxyethyl)-phosphine (TCEP) were from Aldrich. Acetonitrile (AcCN) and trifluoroacetic acid used in HPLC were HPLC grade. All other reagents were analytical grade.

Purification of HWTX-II

HWTX-II was purified from the venom of *S. huwena* by ion-exchange chromatography and reverse-phase HPLC as described by Shu *et al*. [1].

Mass spectrometric analysis

MALDI-TOF MS spectra were recorded on a Bruker Proflex III mass spectrometer. The matrix used was a saturated solution of CCA in AcCN/water (1 : 1). The peptide sample (2 μL, about 1–5 pmol·μL^{-1}) dissolved in a 0.1% trifluoroacetic/water (1 : 2) was mixed with 10 μL of the matrix saturated solution and 2 μL of this mixture was deposited on the target and dried. Spectra were calibrated with internal stands of HWTX-II (4284.19 Da) and trypsin autolysis fragments of 2163.06 Da or 2273.11 Da.

Protein fragmentation with trypsin

Native HWTX-II was digested at 37 °C with Tos-Phe-CH_2Cl/trypsin in 20 mM NH_4HCO_3 at pH 8.0, pH 6.5 or pH 5.0. The course of digestion was monitored periotically by MALDI-TOF MS. At appropriate times, samples were separated by reversed phase HPLC for MS and sequence analysis.

Attachment of HWTX-II to the AP glass

HWTX-II (5 nmol) was dissolved in 30 μL of 1.0 M HCl/pyridine buffer (pH 4.5) in tube A. A 20-μL aliquot of the same buffer was added into tube B containing 1 mg AP glass beads. The two tubes were precooled in an ice bath for 15 min and the contents of tube A and about 1 mg EDC were added to tube B. The mixture in tube B was agitated and allowed to react for 15 min in the ice bath. The glass beads were washed five times with 200 μL methanol by centrifuging the mixture and carefully pipetting off the supernatant liquid.

Edman degradation sequencing

The AP glass beads with coupled HWTX-II were added to the center of the sequencing membrane seal and covered with another membrane seal. The sandwich was then fixed in the cartridge and then put in the reaction chamber of an Applied Biosystem Model 475 gas-phase sequencer. The Edman degradation was performed with a normal automatic cycle program.

In situ modification of free thiol groups by 4-vinylpyridine (4-VP)

Sequencing was interrupted after selected cysteine cycle had finished and the AP-glass bearing the truncated HWTX-II was carefully transferred into microcentrifuge tube. To the tube were added 200 μL AcCN, 2 μL methanol and 2 μL 4-VP. The contents of the tube were mixed and pyridylethylation of the immobilized peptide was allowed to proceed for 1 h at 45 °C. The beads were then washed five times with 200 μL portions of methanol, allowed to dry and returned to reaction chamber, after which sequencing was continued.

RESULTS AND DISCUSSION

Pth analysis during Edman degradation of the native HWTX-II

Signals for Pth–Cys and the Pth of dehydroalanine (ΔSer) were observed in all cysteine cycles during Edman degradation of the native HWTX-II. In case the signals of Pth–ΔSer of Cys4 and Cys8 were disturbed by the Ser5 and Ser7, only Pth–Cys signals were attended in subsequent analysis. The relative yields of Pth–Cys of 37 cycles are shown in the Panel A of Fig. 2. The signal of Pth–Cys in cycle 4 was obvious. Pth signal of Cys and ΔSer of cycle number 8, 18, 23, 29 and 34 can be identified by comparing with that of the former cycle. The result indicated that the disulfide bonds were partially split when the ATZ-Cys decomposed from the peptide chain and then the free thiol group of the second half cystine should be generated. It provided possibility for modification of the nascent thiols in our method.

Analysis of the first disulfide bond of HWTX-II

Pth–Cys and Pth–ΔSer were observed in the chromatogram at the fourth cycle after Edman degradation of HWTX-II immobilized on the AP-glass beads. At the end of the fourth

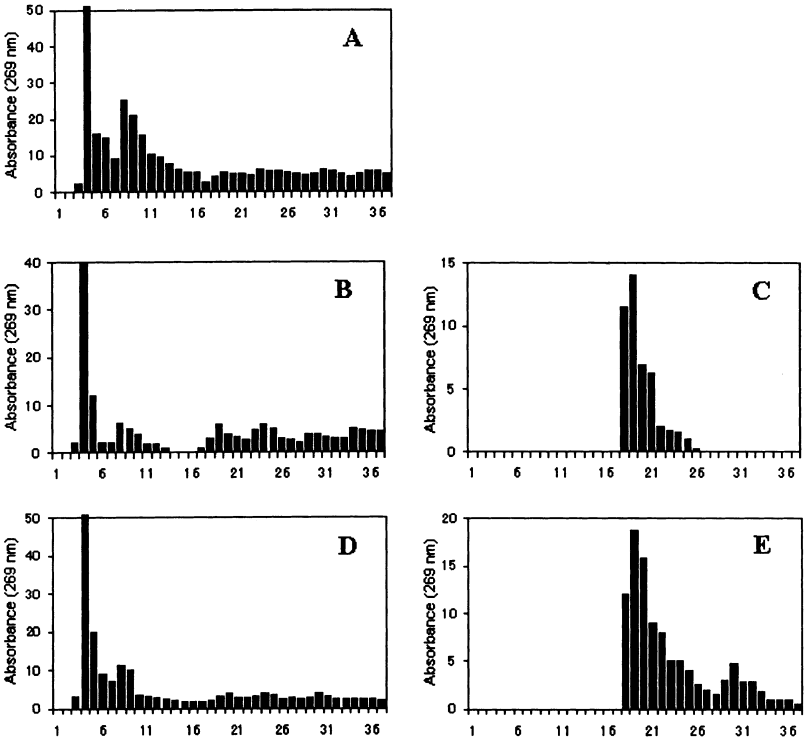

Fig. 2. Pth–Cys and Pth–PECys profiles from sequencing of HWTX-II. The abscissa indicates the yields of Pth–Cys or Pth–PECys at each cycle. The ordinate is the amino-acid residue number for HWTX-II, starting from the N-terminus. (A) Pth–Cys yields for the intact HWTX-II. Pth–Cys signals are above background in all cysteine cycles. (B) Pth–Cys profile for a sample that was alkylated with 4-VP after sequencing through the first Cys residue (cycle 4). (C) Pth–PECys profile for the same sample as in B. Pth–PECys is first seen at cycle 18, indicating that Cys 18 and Cys 4 were disulfide linked in HWTX-II. (D) Pth–Cys analysis of the sample that was alkylated after cycles 4 and 8. (E) Pth–PECys profile of same sample as in D, showing new peaks at cycles 18 and 29.

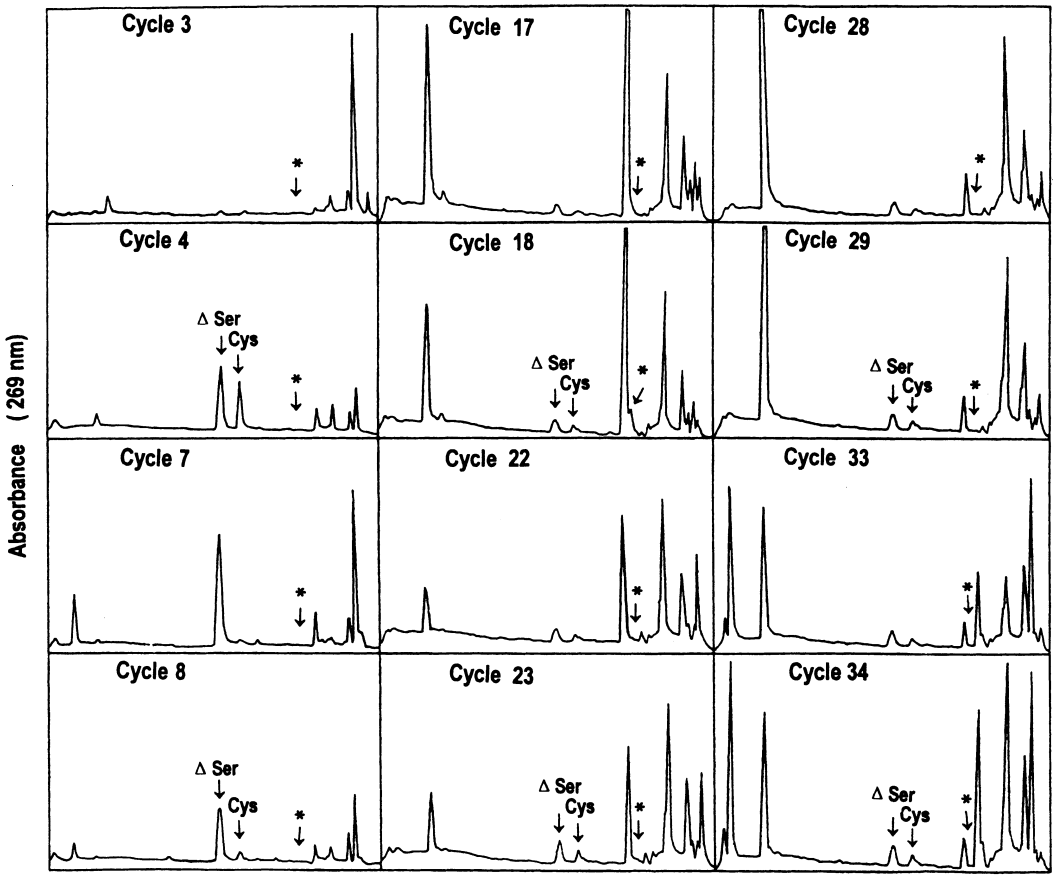

Fig. 3. HPLC profiles of sequencing samples before and after modification with 4-VP after cycle 4. Cys residues occur at cycles 4, 8, 18, 23, 29 and 34. Profiles of the preceding cycles are included for contrast. The elution position of Pth–PECys is marked with an asterisk (*). Nevertheless, a small Pth–PECys peak is seen at cycle 18.

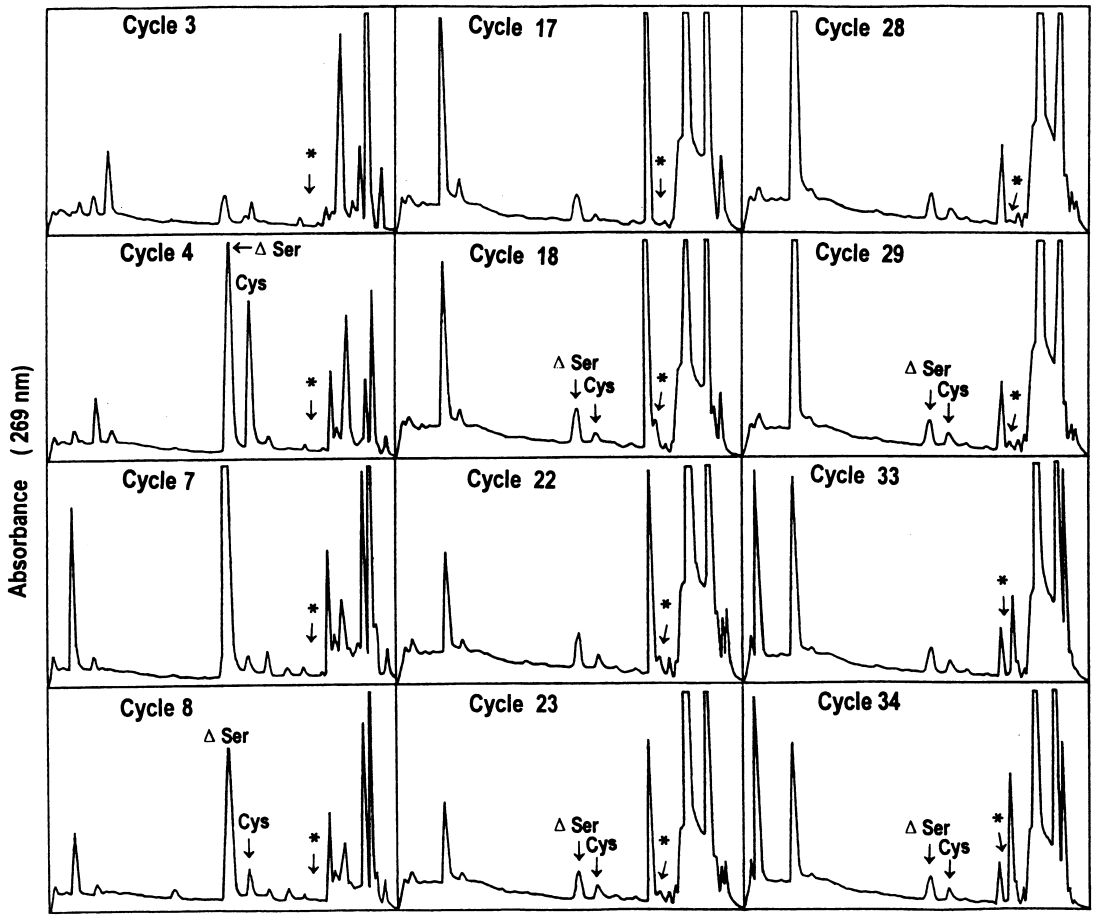

Fig. 4. HPLC profiles of sequencing samples before and after modification with 4-VP after cycle 4 and cycle 8. Conditions as in Fig. 3. Small Pth–PECys peaks are seen in cycle 18 and 29.

cycle, sequencing was halted and the sample was removed from the reaction chamber and alkylated with 4-VP. The sequencer was restarted and sequencing was continued to the end of the peptide. The yields of Pth–Cys and Pth–PECys are compared in panel B and C of Fig. 2, respectively, and the HPLC profiles of the cysteine cycles and their preceding cycles are shown in Fig. 3. A Pth–PECys signal is observed only in cycle Cys18 (Fig. 2C), although both Pth–Cys and Pth–ΔSer are seen in cycles of Cys8, 18, 23, 29 and 34. These results indicate that Cys4 is linked to Cys18 by a disulfide bond.

Analysis of the second disulfide bond of HWTX-II

After the first disulfide was established as Cys4–Cys18, the same procedure was used to analyze the second disulfide, Cys8-CysX (where X would be one of the numbers 23, 29 or 34). Another sample of HWTX-II was sequenced to the C-terminus, with interruptions after cycle 4 and 8 for alkylation with 4-VP. The yields of Pth–Cys and Pth–PECys are compared in panels D and E of Fig. 2, respectively, which show the presence of PECys at cycle 29, as well as at cycle 18. The HPLC profiles of the cysteine and preceding cycles are shown in Fig. 4. Though weak signals for PECys were observed in cycles 23 and 34, it was easy to deduce from the profile that they result from carryover from previous cycles. These data indicate that the second disulfide pair is Cys8–Cys29. By process of elimination, then, the third disulfide must be between Cys23 and Cys34.

The above method is effective for the assignment of disulfide bonds in peptides and small proteins which containing fewer than about 50 residues, the limiting factor being how far into the peptide one can sequence in a single run. The number of sequencing runs required is $n - 1$, where n is the number of disulfide bonds in the peptide.

MALDI-TOF mass analysis of the tryptic fragments of HWTX-II

To confirm the above disulfides for HWTX-II, we carried out a mass spectrometric analysis of the tryptic fragments of native HWTX-II. Typical MALDI TOF MS maps of the tryptic fragments of HWTX-II are shown in Fig. 5. Analysis of peaks observed in Fig. 5 is summarized in Table 1. The appearance of major peaks at *m/z* 2456, 2584, 1648, 1516 and 988 supports the disulfide linkage pattern of 1–3, 2–5 and 4–6 (cf. Table 2.)

The MS maps of the trypsin digest of HWTX-II change with hydrolysis time (Fig. 5). Little proteolysis occurred during the first two hours (Fig. 5A,B), but some disulfide scrambling was observed after 3 h, as indicated by the appearance of a peak at *m/z* 3156.7 (1–3, 2–6; Table 1).

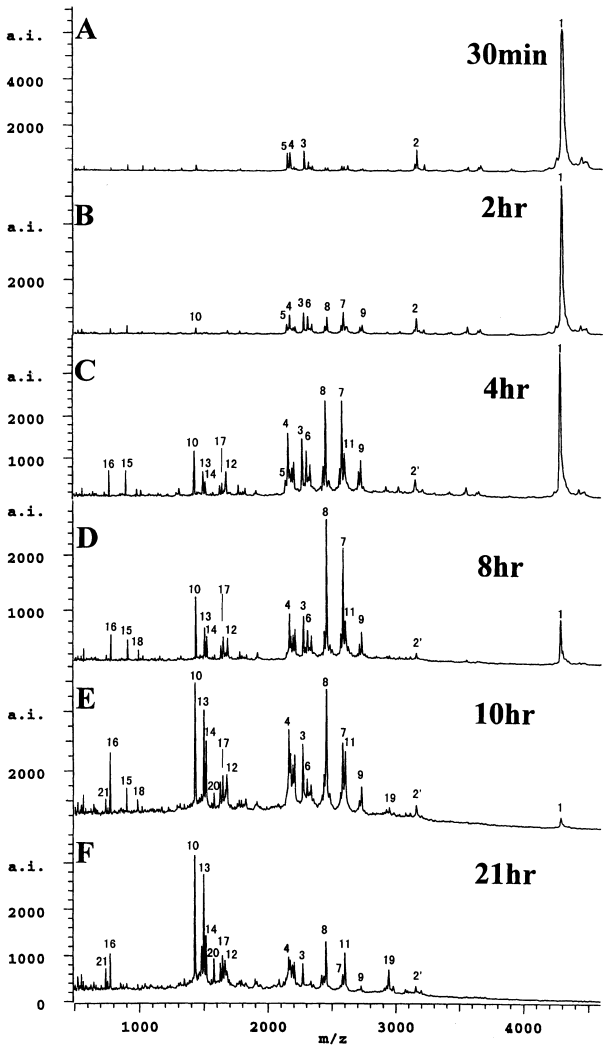

Fig. 5. Time course of trypsinolysis of HWTX-II analyzed by MALDI-TOF MS. Samples of the trypsin digest were analyzed at the indicated times. The average *m/z*-values (± 1) of the numbered peaks are as follows: 1, 4284 (intact HWTX-II); 2, 3156; 2′, 3159~3160; 3, 2273; 4, 2163; 5, 2142; 6, 2306; 7, 2584; 8, 2455; 9, 2730; 10, 1434; 11, 2604; 12, 1681; 13, 1500; 14, 1518; 15, 904; 16, 776; 17, 1648; 18, 988; 19, 2947; 20, 1579; 21, 741. (see also Table 1) Peaks 3, 4, 5, 6, 11 and 20 are trypsin autolysis products.

Appreciable hydrolysis had occurred by 4 h and fragments with the original disulfide arrangement were seen at *m/z* 2456 and 2584 (1–3, 2–5) and 988 and 1517 (4–6). During hours 4 through 10 (Fig. 5C–E; Table 1). Trypsin digestion of HWTX-II was essentially complete after 12 h; longer digestion times let to increased disulfide scrambling. As shown in panel F of Fig. 5 (21h digestion), the size of peaks with native disulfides decreased relative to peaks resulted from disulfide interchange such as at 2947.4 (1–3, 2–6). These results illustrate the value of MS mapping to monitor proteolysis.

The tryptic maps of HWTX-II also varied according to pH. The interchange peaks with disulfide pairs 1–3, 2–6 were higher at pH 8.0 than at pH 6.5. At sufficiently low pH (pH 5.0), there was no proteolysis, even after 18 h (data not shown).

Disulfide exchange in HWTX-II was not random. It was found that the disulfide exchange occurred mainly between fragment (1–3, 2–5) and (1–3, 2–6), i.e. Cys8 (C2)–Cys29 (C5) and Cys8 (C2)–Cys34 (C6), respectively. It may be that Cys8, linked to Cys29 in the native state, is rather close to Cys34, and that in the early stages of proteolysis, cleavage occurs in such a way as to 'loosen' the molecule and favor the (2–5) to (2–6) interchange, resulting in the peak at *m/z* 3156.7 (1–3, 2–6) produced in the early digestion (3 h). Secondly, the scrambling seen at the longer times (after 12 h) seems to be caused by disulfide dismutation, although the main scrambling fragment at *m/z* 2947.4 still has the same disulfide pattern (1–3, 2–6) as the fragment at *m/z* 3156.7. The fragments containing Cys23 (C4) and Cys29 (C5) were both the dipeptide (CK), and the scrambling fragment at *m/z* 2947.4 [(13–19)-SS-(1–12)-SS-(31–36)] was more symmetric than the native fragment, *m/z* 2455.8 [(13–19)-SS-(1–12)-SS-(29–30)]. The disulfide interchange reaction seems to favor generation of symmetrical disulfides, and extended digestion times increase dismutation. Furthermore, cyclic disulfides may be intermediates leading to disulfide exchange. For example, the peak at *m/z* 1433 may represent fragment 1–12 (which contains C1 and C2 in either acyclic(*m/z* 1434.6) or cyclic(*m/z* 1432.6) form, and the peak at *m/z* 1500, the acyclic(*m/z* 1499.8) or cyclic (*m/z* 1497.8) form of fragment 25–36, which contains C5 and C6 (cf. Table 1 and Fig. 5).

This analysis illustrates the limitation of fragmentation/mass spectrometry for the analysis of disulfide bond structure. As disulfide interchange peaks appear early in during proteolysis, it would be difficult to decide which is the correct linkage based on these data alone.

Disulfide linkage pattern of HWTX-II

The disulfide linkage pattern of HWTX-II (1–3, 2–5 and 4–6) (Fig. 6) is rarely reported. HWTX-I [12,13], a neurotoxin, and SHL-I [14,15], a lectin-like peptide, both purified from the venom of the same spider *S. huwena*, have the same disulfide linkage pattern, namely, 1–4, 2–5 and 3–6. HWTX-I and SHL-I shared the same 'cystine knot' motif seen in ω- and μ-agatoxins, ω-conotoxins, gurmarin, the cyclic peptide kalata B1 and circulin A [4,6]. The secondary structural elements are organized around the three disulfides that largely participate in the protein core. The two disulfide bridges (corresponding to C2–C5 and C3–C6) and triple-strand β sheet of the cystine knot motif are similar to those in the CSH (cystine-stabilized α-helical) motif found in hormonal peptides from the endothelin family, apamin, scorpion toxins and insect defensins [16]. It has been pointed out that the disulfide bridge, C2–C5, which crosses the macrocycle formed by the other disulfide bridges (C1–C4 and C3–C6 or others), contributes to the stability of the β sheet and tends to be conserved [16].

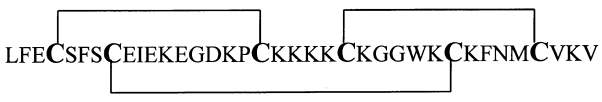

Fig. 6. Deduced disulfide bonding pattern of HWTX-II.

Table 1. Analysis of main peaks appeared in the MALDI-TOF MS map.

Mass observed (*m/z*, ± 1)	Mass calculated (*m/z*)	Fragments of HWTX-II containing Cys resulting from trypsin digestion [d]	Disulfide linkage
3160	3160.7 or 3159.6	(1–12)-SS-(23–37) or (1–19)-SS-(29–36)	1-SH, 2–5,4–6 1–3,2–5, 6-SH [a]
3156	3156.7	(1–20)-SS-(31–37)	1–3, 2–6 [b]
2947	2947.4	(13–19)-SS-(1–12)-SS-(31–36)	1–3, 2–6 [b]
2731	2730	(13–21)-SS-(1–12)-SS-$C_{29}K$ + H_2O	1–3, 2–5 [a]
2713	2712	(13–21)-SS-(1–12)-SS-$C_{29}K$	1–3, 2–5 [a]
2584	2583.9	(13–20)-SS-(1–12)-SS-$C_{29}K$	1–3, 2–5 [a]
2455	2455.8	(13–19)-SS-(1–12)-SS-$C_{29}K$	1–3, 2–5 [a]
1681	1681.9	(1–12)-SS-$C_{29}K$	2–5, 1-SH [a]
1648	1648	(25–36)-SS-$C_{23}K$	4–6, 5-SH [a]
1629	1630	23–36	4–6, 5-SH [a]
1519	1518.6	(1–6)-SS-(13–19)[c]	1–3 [a]
1517	1515.8	(23–28)-SS-(31–37)	4–6 [a]
1500	1497.8 or 1499.8	25–37	5-SH, 6-SH or 5–6 [b]
1433	1434.6 or 1432.6	1–12	1-SH, 2-SH or 1–2 [b]
988	988.2	$C_{23}K$-SS-(31–36)	4–6 [a]
904	904	13–20	3-SH
776	775.8	13–19	3-SH
740	740.9	31–36	6-SH

[a] Native fragment; [b] interchange fragment; [c] 'pseudotryptic' fragments; [d] the subscript numbers refer to the position of the cysteine residue in the peptide sequence.

The second disulfide in HWTX-II (C2–C5) is the same as that in HWTX-I and SHL-I, which crosses two macroloops formed by the first (C1–C3) and third (C4–C6) disulfides. Therefore the disulfide (C2–C5) crossing the macrocycle formed by the other disulfide bridges and interconnecting backbone is presumed to be the most important, and presumably is the reason it is conserved. This assignment and analysis of the disulfide bonds of HWTX-II will be helpful in future studies of the structure and the relationship between structure and function of the molecule.

ACKNOWLEDGEMENTS

This work was supported by the National Natural Sciences Foundation of China under contract no. 3990600.

Table 2. Analysis of the trypsin digesting fragments relating with disulfide pattern of HWTX-II. The fragments including Cys are 1–12 ($LFEC_4SFSC_8EIEK$, 1434.6 Da), 13–19 ($EGDKPC_{18}K$, 775.9 Da), 23–24 ($C_{23}K$, 249.3 Da) and 29–30 ($C_{29}K$, 249.3 Da) and 31–36 ($FNMC_{34}VK$, 740.9 Da). Pattern 1 and 2 are the same in characters of sequence and mass. So are: patterns 4, 5, 7 and 10; patterns 6 and 13; patterns 8 and 11; patterns 9, 12, 14 and 15. Only pattern 3 is unique.

No	Pattern	Fragments Sequence	Mass
1	1–2, 3–4, 5–6	(1–12) (13–19)-SS-$C_{23}K$, $C_{29}K$-SS-(31–36)	1432.6, 1023.2, 988.2
2	1–2, 3–5, 4–6	(1–12) (13–19)-SS-$C_{29}K$, $C_{23}K$-SS-(31–36)	1432.6, 1023.2, 988.2
3	1–2, 3–6, 4–5	(1–12) (13–19)-SS-(31–36), $C_{23}K$-SS-$C_{29}K$	1432.6, 1514.8, 446.6
4	1–3, 2–4, 5–6	(13–19)-SS-(1–12)-SS-$C_{23}K$, $C_{29}K$-SS-(31–36)	2455.8, 988.2
5	1–3, 2–5, 4–6	(13–19)-SS-(1–12)-SS-$C_{29}K$, $C_{23}K$-SS-(31–36)	2455.8, 988.2
6	1–3, 2–6, 4–5	(13–19)-SS-(1–12)-SS-(31–36), $C_{23}K$-SS-$C_{29}K$	2947.4, 496.6
7	1–4, 2–3, 5–6	$C_{23}K$-SS-(1–12)-SS-(13–19), $C_{29}K$-SS-(31–36)	2455.8, 988.2
8	1–4, 2–5, 3–6	$C_{23}K$-SS-(1–12)-SS-$C_{29}K$ (13–19)-SS-(31–36)	1929.2, 1514.8
9	1–4, 2–6, 3–5	$C_{23}K$-SS-(1–12)-SS-(31–36),(13–19)-SS-$C_{29}K$	2420.8, 1023.2
10	1–5, 2–3, 4–6	$C_{29}K$-SS-(1–12)-SS-(13–19), $C_{23}K$-SS-(31–36)	2455.8, 988.2
11	1–5, 2–4, 3–6	$C_{29}K$-SS-(1–12)-SS-$C_{23}K$ (13–19)-SS-(31–36)	1929.2, 1514.8
12	1–5, 2–6, 3–4	$C_{29}K$-SS-(1–12)-SS-(31–36),(13–19)-SS-$C_{23}K$	2420.8, 1023.2
13	1–6, 2–3, 4–5	(31–36)-SS-(1–12)-SS-(13–19),$C_{23}K$-SS-$C_{29}K$	2947.4, 496.6
14	1–6, 2–4, 3–5	(31–36)-SS-(1–12)-SS-$C_{23}K$ (13–19)-SS-$C_{29}K$	2420.8, 1023.2
15	1–6, 2–5, 3–4	(31–36)-SS-(1–12)-SS-$C_{29}K$ (13–19)-SS-$C_{23}K$	2420.8, 1023.2

REFERENCES

1. Shu, Q. & Liang, S. (1999) Purification and characterization of huwentoxin-II, a neurotoxic peptide from the venom of the Chinese bird spider *Selenocosmia huwena*. *J. Pept. Res.* **53**, 486–491.
2. Anette, S.N. (1989) Tarantula (*Eurypelma californicum*) venom, a multicomponent system. *Biol. Chem. Hoppe-Seyler* **370**, 485–498.
3. Kaiser, I.I., Griffin, P.R., Aird, S.D., Hudiburg, S., Shabanowitz, J., Francis, B., John, T.R., Hunt, D.F. & Odell, G.V. (1994) Primary structures of two proteins from the venom of the Mexican red knee tarantula (*Brachypelma smithii*). *Toxicon* **32**, 1083–1093.
4. Pallaphy, P.K., Nielsen, K.J., Craik, D.J. & Norton, R.S. (1994) A common structural motif incorporating a cystine knot and a triple-stranded β-sheet in toxic and inhibitory polypeptides. *Protein Sci.* **3**, 1833–1839.
5. Omecinsky, D.O., Holub, K.E., Adams, M.E. & Reily, M.D. (1996) Three dimensional structure analysis of μ-agatoxins: further evidence for common motifs among neurotoxins with diverse ion channel specificities. *Biochemistry* **35**, 2836–2844.
6. Norton, R.S. & Pallaghy, P.K. (1998) The cystine knot structure of ion channel toxins and related polypeptides. *Toxicon* **36**, 1573–1583.
7. Gray, W.R. (1993) Disulfide structure of highly bridged peptides: a new strategy for analysis. *Protein Sci.* **2**, 1732–1748.
8. Gray, W.R. (1993) Echistatin disulfide bridges: selective reduction and linkage assignment. *Protein Sci.* **2**, 1749–1755.
9. Wu, J. & Watson, J.T. (1997) A novel methodology for assignment disulfide bond pairings in proteins. *Protein Sci.* **6**, 391–398.
10. Bures, E.J., Hui, J.O., Young, Y., Chow, D.T., Katta, V., Rohde, M.F., Zeni, L., Rosenfeld, R.D., Stark, K.L. & Haniu, M. (1998) Determination of disulfide structure in Agouti-related protein (AGRP) by stepwise reduction and alkaylation. *Biochemistry* **37**, 12172–12177.
11. Nokihara, K., Morita, N., Yamaguchi, M. & Watanabe, T. (1992) Sequence analysis of cysteine and cystine containing peptides and proteins by a gas-phase sequencer with isocratic separation of PTH-amino acids. *Anal Lett* **25**, 513–533.
12. Zhang, D. & Liang, S. (1993) Assignment of the three disulfide bridges of Huwentoxin-I, a neurotoxin from the spider *Selenocosmia huwena*. *J. Protein Chem.* **12**, 735–740.
13. Qu, Y., Liang, S., Ding, J., Liu, X., Zhang, R. & Gu. X. (1997) Proton nuclear magnetic resonance studies on huwentoxin-I from the venom of the spider *Selenocosmia huwena*: 2. Three-dimensional structure in solution. *J. Protein Chem.* **16**, 565–574.
14. Li, F. & Liang, S. (1999) Assignment of the three disulfide bonds of *Selenocosmia huwena* lectin-I from the venom of spider *Selenocosmia huwena*. *Peptides* **20**, 1027–1034.
15. Lu, S., Liang, S. & Gu, X. (1999) Three-dimentional structure of *Selenocosmia huwena* lectin-I from the venom of the spider *Selenocosmia huwena*. *J. Protein Chem.* **18**, 609–617.
16. Heitz, A., Le-Nguyen, D. & Chiche, L. (1999) Min-21 and Min-23, the smallest peptides that fold like a cystine-stabilized β-sheet motif: design, solution structure, and thermal stability. *Biochemistry* **38**, 10615–10625.